AUTOMATED DETECTING ARCUS SENILIS, SYMPTOM FOR CHOLESTEROL PRESENCE USING IRIS RECOGNITION ALGORITHM

R.A.Ramlee, K.A.Aziz, S.Ranjit, Mazran Esro

Faculty of Electronic and Computer Engineering
Universiti Teknikal Malaysia Melaka

Email: ridza@utem.edu.my

Abstract

Arcus senilis is a whitish ring-shaped or bow-shaped deposit in the cornea. It is recognized as a sign of hyperlipidemia and is also associated to coronary heart disease (CHD). Iridology is an alternative method to detect diseases using iris's pattern observation. Iridologists believe that the whitish deposit on the iris is sign of heart diseases. We develop the simple and non-intrusive automation system to detect cholesterol presence using iris recognition (image processing). This system applies iris recognition method to isolate the iris area, normalization process and lastly determining the cholesterol presence using OTSU histogram method to determine the threshold value. The result showed that the incidence of cholesterol was high when eigen value exceeds a threshold value.

Keywords: Iris recognition, biometric identification, iridology, Arcus Senilis, Corneal arcus, cardio diseases.

I. INTRODUCTION

Iris is a pigmented, round, contractile membrane of the eye, suspended between the cornea and lens and perforated by the pupil depicted in Fig. 1. It regulates the amount of light entering the eye [1]. According to [2], the eyes are connected and continuous with the brain's Dura mater through the fibrous sheath of the optic nerves, and they are connected directly with the sympathetic nervous system and spinal cord. The optic tract extends to the thalamus area of the brain. This creates a close association with the hypothalamus, pituitary and pineal glands. These endocrine glands, within the brain, are major control and processing centres for the entire body. Because of this anatomy and physiology, the eyes are in direct contact with the biochemical, hormonal, structural and metabolic processes of the body. This information is recorded in the various structures of the eye, i.e. iris, retina, sclera, cornea, pupil and conjunctiva. Thus, it can be said that the eyes are a reflex or window into the bioenergetics of the physical body and a person's feelings and thoughts [2]. There are a lot of arguments between iridologists (iridology's practitioner) and the medical's practitioner. Due to this argument, numerous studies done by the medical's practitioner found that the diagnosis done by the iridologist upon the patient is not accurate. Another study on iris changes in related with disease, carried out in the research of ocular complication of adult rheumatoid arthritis done by [3], found that the mean duration of the arthritis and the mean duration of seropositivity were found to be significantly higher in patients with ocular (pigmented organ in eye) complication [3]. Another study done on bilateral retinal detachment in acute myeloid leukaemia by [4], found that ocular manifestations are common in patient with acute leukaemia. This can result from direction infiltration by neoplastic cells of ocular tissues, including optic nerve, choroid, retina, iris and ciliary body, or secondary to hematology abnormalities such as anemia, thrombocytopenia, or hyperviscosity states or retinal destruction by opportunistic infection [4]. The history of Iridology study on iris was done by the physician Philippus Meyens in 1670 in his book Chromatica Medica, explaining

the features of the iris (iridology). In the book he stated that the eye (iris) contains valuable information about the body. In 1881 a Hungrarian physician, Dr. Ignatz Peczley introduced the first chart of the iris explaining zone in the iris [2]. The idea begun when he found a dark scar in the Owl's iris scar turned white as the leg healed.

The objective of this project is to explain how the presence of cholesterol in blood vessel can be detected by using iris recognition algorithm. This method used the [5], [6] iris recognition methods and extends the study of eyes pattern to other application and in this case, the alternative medicine that is iridology

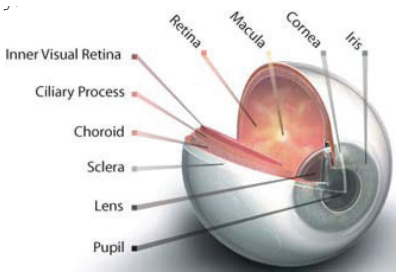

Fig. 1: Human Eye Anatomy

IIris recognition is one of the most widely implemented biometric systems in use today. John Daugman is said to have developed the most widely used algorithms and most efficient methods of recognition, but there have been many new findings and algorithms [7]. Reference [5] has verified the uniqueness of human iris patterns and developed an open source iris recognition system.

Based on the iris recognition methods and iridology chart, a MATLAB program has been created to detect the present of cholesterol in our body.

Cholesterol or Hypercholesterolemia is a high level of lipid in the blood poses a significant threat to person's health. It is an indication of elevated cholesterol which may lead to cardiovascular diseases. It is caused by extracellular lipid deposition in the peripheral cornea, with the deposits consisting of cholesterol, cholesterol esters, phospholipids, and triglycerides. The fatty acids that make up many of the deposited lipid molecules include palmitic, stearic, oleic, and linoleic acids [8].

The current technique used to measure the cholesterol level is by doing blood test and the test is known as lipoprotein profile. The lipoprotein profile is an invasive method which causes discomfort amongst many patients. Reference [9] introduced a laser based technology as non-invasive technique to measure blood cholesterol through skin. They proposed infrared (IR) absorption spectroscopic as the characterization of cholesterol in the skin. Based on [10], skin contains approximately 11 percent by weight of all body cholesterol and when severe coronary artery disease is present, the numeric values obtained with the skin cholesterol test increases. Thus, the palm test is not useful in identifying coronary artery disease and it is not intended to be used as a screening tool to determine the risk for coronary artery disease in general population.

In order to have a simple and non-intrusive means to be as a screening tool to detect cholesterol, we have considered alternative medicines. Iridology is one of the alternative medicines, which claims that iris pattern could reflect one's health and reveal the state of individual organs. According to iridology, cholesterol in body can be detected if there is a "sodium ring" in the patient's eyes. However, since there were statements that regard iridology as medical fraudulent [6] we were looking at other medical statements that can relate cholesterol and other organs. We found out that high cholesterol can be detected from changes in iris pattern and they are called Arcus Lipoides (Arcus Senilis or Arcus Juvenilis). Arcus senilis is a greyish or whitish arc or circle visible around the peripheral part of the corner in older adults. Arcus senilis is caused by lipid deposits in the deep layer of the peripheral cornea and not necessarily

associated with high blood cholesterol. However, similar discoloration in the eyes of younger adults (arcus juvenilis) is often associated with high blood cholesterol [11]. This statement proves that iris pattern can be analyzed and used as another technique to detect cholesterol presence in body.

Reference [12], conclude in his study the presence of Arcus Senilis before the age of 56 and large wrist size were found to appear with a frequency in coronary group which made their presence statistically significant at level 5%. Hypercholesterolemia was common finding in coronary patient who demonstrated Arcus Senilis and greying of hair. According to [11] although iridology has been criticized as an unfounded diagnostic tool, many iridologists are presently practicing in many areas. In Germany, 80% of Heilpraktiker (non-medically qualified health practitioners) practice iridology [13]. In this study, [11] investigated the ACE genotypes of hypertensive patients classified by their iris constitutions. As a result, 74.7% of hypertensive patients were neurogenic or cardio-renal connective tissue weakness type. Also, the frequencies of DD genotype were significantly higher in hypertensive patients than in controls. These results are consistent with the reports that DD genotype was associated with hypertension. Therefore, [11] present the results support that D allele is a candidate gene for hypertension, and suggest an apparent relationship between ACE genotype and iris constitutions, as well as the novel possibility of molecular genetics understanding of iridology.

II. EYE IMAGE

The eye is the organ of sight, a nearly spherical hollow globe filled with fluids (humors). The outer layer or tunic (sclera, or white, and cornea) is fibrous and protective. The middle tunic layer (choroid, ciliary body and the iris) is vascular. The innermost layer (the retina) is nervous or sensory. The fluids in the eye are divided by the lens into the vitreous humor (behind the lens) and the aqueous humor (in front of the lens). The lens itself is flexible and suspended by ligaments which allow it to change shape to focus light on the retina, which is composed of sensory neurons (NLM, 2010). Fig. 1 shows the anatomy of human eye which contain the area of sclera and iris for references. The iris image needs to be extracted from the original eye image. This solid iris image is used in this system to verify the presence of cholesterol. Thus it is vital to isolate this part (iris) from the whole unwanted part in the eye (sample). This separation or segmentation is the process of remove the outer part of the eye (outside the iris circle), in order to get solid image of iris that useful for localisation the cholesterol lipid. Generally this eye breaks up into two parts, the first part is the inner region which is the iris and pupil boundary and the second part is the outer regions, the iris and sclera boundary. The quality of the images is very important to get the best result, thus the images should not have any impurities that can cause miss localization. These impurities include the flash reflection from camera and wrong angle of image capture.

In this project the sample of eye is very important because analysis base on the data from human eyes. For this work, we focus on the detecting arcus senilis using iris recognition algorithm and not focusing of method to extract the iris images. Therefore, we use images obtained freely from a few free database sources that can found in website, these databases such as UBIRIS, UPOL, MMU and CASIA [14-17].

UBIRIS [14] database is comprised of 1877 images collected from 241 subjects within the University of Beira Interior 6 in two distinct sessions and constituted, at its release date, the world's largest public and free iris database for biometric purposes.

In CASIA [17], iris image database includes 756 iris images from 108 eyes, hence 108 classes. For each eye, 7 images are captured in two sessions, where three samples are collected in the first and four in the second session. Similarly to the above described database, its images were captured within a highly constrained capturing environment, which conditioned the characteristics of the resultant images. They present very close and homogeneous characteristics and their noise factors are exclusively related with iris obstructions by eyelids and eyelashes (Fig. 2). Moreover, the post process of the images filled the pupil regions with black pixels, which some authors used to facilitate the segmentation task.

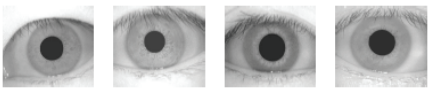

Fig. 2: Examples of iris images from the CASIA [17] database.

The Multimedia University has developed a small data set of 450 iris images MMU [16]. These images were captured using LG IrisAccessR 2200 camera. This is a semi-automated camera that operates at the range of 7-25 cm. Obviously, the images are highly homogeneous and their noise factors are exclusively related with small iris obstructions by eyelids and eyelashes (Fig. 3).

Fig. 3: Examples of iris images from the MMU [16] database.

For this project the difficulty is to achieve the subject or patient to get real image of eye sample, the best place to get these real eye images is at ophthalmology department since this department deal with various case of eye problem that later can be refer to *Arcus Senilis* problem. For this reason, the samples only can be used from free source medical website. Fig. 4 shows a few samples from medical website such as National Library of Medicine and Mediscan clipart library.

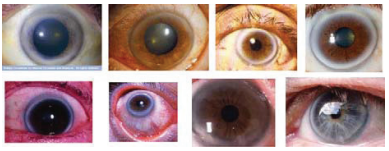

Fig. 4: Examples of iris images from medical website.

III. HOUGH TRANSFORM

The Hough transform is a standard computer vision algorithm that can be used to determine the parameters of simple geometric objects, such as lines and circles, present in an image. The circular Hough transform can be employed to deduce the radius and centre coordinates of the pupil and iris regions. An automatic segmentation algorithm based on the circular Hough transform is employed [18]. Firstly, an edge map is generated by calculating the first derivatives of intensity values in an eye image and then set the threshold base on the result. From the edge map, votes are cast in Hough space for the parameters of circles passing through each edge point. These parameters are the centre coordinates xc and yc, and the radius r, which are able to define any circle according to the equation

$$x_c^{\,2} + y_c^{\,2} + r^2 = 0 \qquad (1)$$

A maximum point in the Hough space will correspond to the radius and centre coordinates of the circle best defined by the edge points. References [18], [19] also make use of the parabolic Hough transform to detect the eyelids, approximating the upper and lower eyelids with parabolic arcs, which are represented as;

$$((-x-h_j)\sin\theta_j+(y-k_j)\cos\theta_j)^2 = a_j((x-h_j)\cos\theta_j+(y-k_j)\sin\theta_j) \qquad (2)$$

a_j controls the curvature, (h_j, k_j) is the peak of the parabola and is the angle of rotation relative to the x-axis.

In performing the preceding edge detection step, [18] bias the derivatives in the horizontal direction for detecting the eyelids, and in the vertical direction for detecting the outer circular boundary of the iris. The motivation for this is that the eyelids are usually horizontally aligned, and also the eyelid edge map will corrupt the circular iris boundary edge map if using all gradient data. Taking only the vertical gradients for locating the iris boundary will reduce influence of the eyelids when performing circular Hough transform, and not all of the edge pixels defining the circle are required for successful localisation. Not only does this make circle localisation more accurate, it also makes it more efficient, since there are less edge points to cast votes in the Hough space.

IV. SEGMENTATION

This segmentation (localization) process is to search for the centre coordinates of the pupil and the iris along with their radius. These coordinates are marked as ci, cp, where ci represented as the parameters of [xc,yc,r] of the limbic and iris boundary and cp represented as the parameters of [xc,yc,r] of the pupil boundary. It makes use of [18] to select the possible centre coordinates first. The method consist of threshold followed by checking if the selected points (by threshold) correspond to a local minimum in their immediate neighbourhood these points serve as the possible centre coordinates for the iris. These radius values were set manually, (Table 1) shows the rmin and rmax varies from 75 to 250 where the ranges for iris between 90 to 150 pixels and for pupil radius are 28 to 75 pixels. The input for this function is the image to be segmented and the input parameters in this function including rmin and rmax (the minimum and maximum values of the iris radius). The range of radius values to search for was set manually, depending on the database used. For the CASIA database, rmin is set to 55 pixels and rmax is set to 160 pixels. The sample of Arcus Senilis eye (arcus7.bmp) is downloading from (Mediscan, 2000), for this image the rmin is set to 70 pixels and rmix is set to 260 pixels. Table 1 shows the others sample run for segmentation process.

Table 1: shows the example of the images and their rmin and rmax values.

Image	rmin	rmax
Iris1.bmp (CASIA)	75	260
Iris2.bmp (CASIA)	75	260
Iris3.bmp (CASIA)	75	260
Iris4.bmp (CASIA)	75	260
Iris6.bmp (CASIA)	75	260
c_mo1.bmp	50	83
c_mo2.bmp	75	260
normal1.bmp	75	260
Arcus1.bmp (Medical Web)	80	260
Arcus2.bmp (Medical Web)	80	260
Arcus3.bmp (Medical Web)	80	260
Arcus4.bmp (Medical Web)	80	260
Arcus5.bmp (Medical Web)	80	260
Arcus6.bmp (Medical Web)	80	260
Arcus7.bmp (Medical Web)	80	260
Arcus2.bmp (Medical Web)	80	260
Arcus2.bmp (Medical Web)	80	260
Arcus2.bmp (Medical Web)	80	260
ubiris1.bmp (UBIRIS)	85	260
ubiris2.bmp (UBIRIS)	85	260
ubiris2.bmp (UBIRIS)	85	260

The output of this function will be the value of c_p and c_i, which is the value of $[x_c, y_c, r]$ for the pupilary boundary and the limbic / iris boundary and also the segmented image. The program processes the image from [17] database as shown in the Fig. 5. This image gives wrong detection on pupil boundary because segmentation on pupil is segmented on the illumination light rather than segmented the pupil boundary.

Even though the pupil boundary is not accurately detected in this segmentation process, these images still can be accepted since the incidence of cholesterol normally occur from limbic up to pupil which is 30 percents from overall normalization image. Therefore for this kind of segmentation we consider the correct segmentation of iris boundary rather than pupil boundary segmentation. More

examples for this process will show in the result's section.

Another example as shows in the Fig. 6, fail to determine the edge of pupil but it detect the edge of the impurity illumination light. This will effect to the quality of the segmentation eyes image, cause to imperfectly to detect iris and pupil boundary region of the eyes.

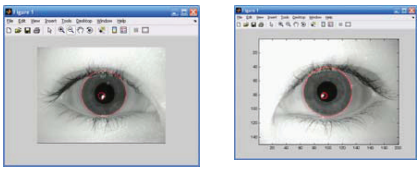

Fig. 5: An example where segmentation fails. The segmentation is failing to detection correctly the edges of the pupil border, but it segmented illumination light.

But luckily the significant area of white ring (*Arcus Senilis*) lay at the boundary of sclera or iris up to the pupil, so as long as the segmentation done correctly on the iris it can considered succeed. This segmentation image will be crop base on the value of iris's radius.

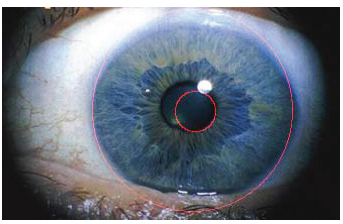

Fig. 6: Another example where segmentation fails to find the edges of the pupil border.

The problem with this image is the existing of illumination from camera (on top of the pupil) will cause inaccurate detection of iris and pupil boundary. This process consider failure if the purpose of this segmentation process is used for biometric iris recognition, but for this system since the image only need to be analyze in 30 percent from the limbic (border of iris) so this result can be used.

V. NORMALIZATION

After the iris is localized, the next step is normalization (iris enrolment). It is a process after localization (segmentation) intends to change the iris region to the fixed form (circle shape) in order to make further analysis. From the process of normalization, the segmented image of the eye will give the value radius pupil and the iris. This image will be cropped base on the value of iris radius, so that the unwanted area will be removed (e.g. sclera and limbic). Therefore only the intended area can be analyzed. According to [8], arcus senilis is described as a yellowish-white ring around the cornea that is separated from the limbus by a clear zone 0.3 to 1 mm in width. Normally the area of white ring (Arcus Senilis), occurs from the sclera/iris up to 20 to 30 percents toward to pupil, so this is the only the main area that have to be analyzed. The other reason to normalize is to make the analysis process become easier rather than to examine the eye in circular shape. In rectangular shape analyze can be done either from top to bottom or from bottom to top. (J. Daugman, 2004) describes details on algorithms used in iris recognition. He has introduced the Rubber Sheet Model that transforms the eye from circular shape into rectangular form and it is shown in Fig.7. This model remaps all point within the iris region to a pair of polar coordinates (r, θ), where θ is the angle [0, 2π] and r is on the interval [0, 1].

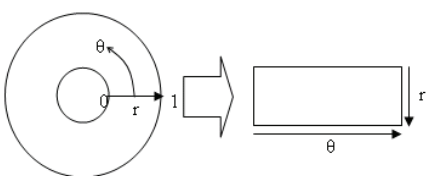

Fig. 7: Daugman's rubber sheet model.

The remapping of the iris image I(x, y) from Cartesian coordinates to the normalized non-concentric polar representation can be modelled as:

$$I(x(r,\theta), y(r,\theta)) \rightarrow I(r,\theta) \quad (3)$$

With

$$x(r,\theta) = (1-r)x_p(\theta) + rx_I(\theta) \quad (4)$$

$$y(r,\theta) = (1-r)y_p(\theta) + ry_I(\theta) \quad (5)$$

Where I(x,y) is the iris region image, (x, y) are the original Cartesian coordinates, (r, θ) are the corresponding normalised polar coordinates, and x_p, y_p and x_I, y_I are the coordinates of the pupil and iris boundaries along the θ direction. The localization of the iris and the coordinate system is able to achieve invariance to 2D position and size of the iris, and to the dilation of the pupil within the iris.

The normalization process is illustrated in Fig. 8. It is done by taking the reference point from the centre of the pupil and radial vectors pass via the iris area. There are two important data points along each radial line which are radial resolution for radial line in pupil and angular resolution for radial line around the iris region. Since the pupil can be non-matching with the iris therefore it need to remap to rescale the points depending to the angle around the iris and pupil. This formula given by:

$$r' = \sqrt{\alpha}\beta \pm \sqrt{\alpha\beta^2 - \alpha - r_I^2} \quad (6)$$

With

$$\alpha = o_x^2 + o_y^2 \quad (7)$$

$$\beta = \cos\left(\pi - \arctan\left(\frac{o_y}{o_x}\right) - \theta\right) \quad (8)$$

The shift of centre of the pupil relative to the iris centre, this given by O_x ,O_y, and r′ is the distance between edge of pupil and edge of the iris at the angle θ around the region, and r′ is the radius of the iris. The remapping formula first gives the radius of the iris region 'doughnut' as a function of the angle θ.

A constant number of points are chosen along each radial line, so that a constant number of radial data points are taken, irrespective of how narrow or wide the radius is at a particular angle. The normalised pattern was created by backtracking to find the Cartesian coordinates of data points from the radial and angular position in the normalised pattern. From the 'doughnut' iris region, normalisation produces a 2D array with horizontal dimensions of angular resolution and vertical dimensions of radial resolution.

The normalisation process proved to be successful and some results are shown in Fig 9. This normalization process will transforms the segmented eye from the circular form to the rectangular shape. However normalisation output will be cropped until 30 percents, from the bottom eye (sclera and iris boundary) toward pupil.

Normalisation of two eye images of the same iris is shown in Fig 9. The pupil is smaller in the bottom image, however the normalisation process is able to rescale the iris region so that it has constant dimension. Note that rotational inconsistencies have not been accounted for by the normalisation process, and the two normalised patterns are slightly misaligned in the horizontal (angular) direction. Rotational inconsistencies will be accounted for in the matching stage.

It is difficult to do analysis if the image is in the original form therefore the image needs to be wrapped to transform the nature from circle to rectangular shape. This process only can be achieved by doing the conversion polar to rectangular. However, the normalisation process was not able to perfectly reconstruct the same pattern from images with varying amounts of pupil dilation, since deformation of the iris results in small changes of its surface patterns.

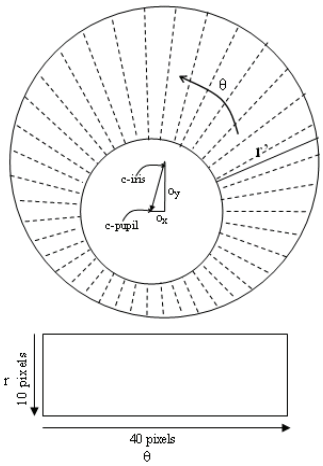

Fig. 8: Outline of the normalization process with radial resolution of 10 pixels, and angular resolution of 40 pixels.

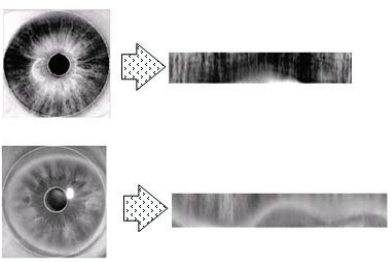

Fig 9: Illustration of the normalization process, normal and illness eye.

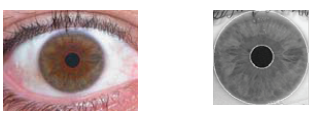

Fig. 10: Color and grey scale eye images using [14] database.

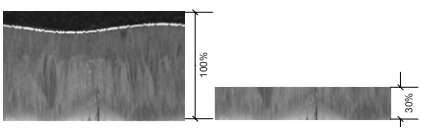

Fig. 11: Stages of normalization 100 percents and 30 percents display after transformation from polar to rectangular.

The normalization process is used for converting the circular iris into rectangular form with fixed dimension as shown in Fig 12. We can see clearly the circle shape (localisation) turn to rectangular shape (normalisation) and also the signs in both pictures are labelled to illustrate the upper eyelid, pupil and white dot exit during segmentation and after normalisation.

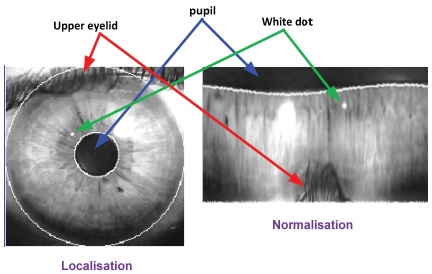

Fig. 12: Stages of normalization.

VI. CHOLESTEROL DETECTION SYSTEM

The process starts with obtaining number of normal eyes and illness eye images (*arcus senilis*).

The next step is to isolate the actual iris region in digital eye image. The isolation process needs to be done to segment the outer boundary for the iris and the inner boundary for the pupil. This can only be done by searching the centre point of the pupil given by x and y axis as propose by [18]. Hough transform [18] is used to detect edge of the iris and pupil circle.

Next, the image has to be analyzed and this can only be done if it is transformed to normalized polar coordinates using Rubber Model. Since the "sodium ring", terminology given in iridology, or arcus senilis for the greyish or whitish arc in iris is only available at the bottom of this coordinate, thus only 30% (Fig.11), of the iris part is considered in the normalization.

Lastly, to determine whether the eye has the ring, histogram of the image has to be plotted so that the decidability can be determined using OTSU's method. The algorithm assumes the image contains two classes of pixels (e.g. foreground and background) and finds the optimum

threshold separating the two classes so that their combined spread (within-class variance) is minimal.

VII. RESULTS

A clear view for this cholesterol detection system demonstrate in Fig. 13 whereas shows the entirely process of the cholesterol detection system using iris recognition and image processing algorithm. This process comprises the following actions:

a) Eye images acquire from database (CASIA, UBIRIS, MMU and medical web) or from digital camera.
b) Process of pupil and iris localization and segmentation, to classify the required region.
c) Attain normalization iris from circular shape to rectangular shape with full image.
d) Crop the normalization iris to 30% from full image, (as shown in Fig.11).
e) Analyze the normalization iris to get the histogram value.
f) Using OTSU to calculate the optimum threshold to detect arcus senilis (Cholesterol presence).
g) Results "Sodium ring detected" or "not detected" will be display in MATLAB window.

For this experiment the boundary value of threshold in the examined eye image is set to 139 (this was decide after run 50 samples of the eye image), the average boundary of the illness or detected eye problem with sign of the presence cholesterol deposited. If the threshold value fallen below this value the eye image is considered as normal (no existing white ring or cholesterol), but if the threshold value rise up beyond this value (139), the subject or patient is detected a sign of the presence of cholesterol. The algorithm is written using MATLAB. The result is based on the value obtained in the automated detecting cholesterol presence (ADCP). The output of algorithm will be either "sodium ring is detected" or "no sodium ring is detected" depend on the sampling eye images processed by the ADCP. By using this ADCP will determine either someone have the symptom of the cholesterol presence or not. The result however is display in command window, but yet this program can be run and display using Graphic User Interface (GUI), where MATLAB has tool to perform it.

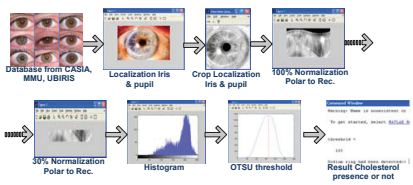

Fig. 13: Overall system for Cholesterol Detection

Fig 15 shows the histogram, threshold values and the statement about the condition of the normal and *Arcus Senilis* iris, respectively. From the histogram and OTSU's method, the decidability or threshold value to distinguish between normal eyes and eyes with *Arcus Lipids* is found to be 139. This value is determined after testing 30 images of normal eyes. If the cluster mean value is less than this threshold, this means than the eye is normal eye and if it is above 139, then the eye can be detected as eye with *Arcus Lipids*.

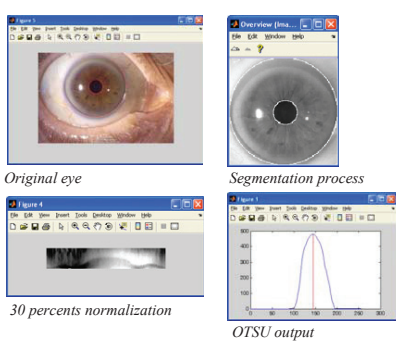

Fig. 14: Stages of localization with eye image 'Arcus1.bmp' from the medical web, (Clock wise from top left) original colour eye image localization, the iris and pupil

detected correctly. (Top right) Gray eye image localization (Bottom left) 30 percents display from polar to rectangular of localization eye with enhancement. (Bottom right) OTSU threshold value for this eye is 144.

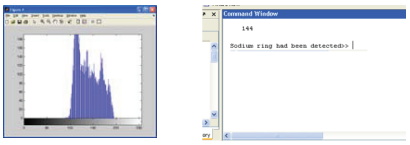

Histogram output *Final result*

Fig. 15: Results from eye with "sodium ring' or Arcus senilis i.e. 'arcus1.bmp': histogram, threshold value and statement of iris condition

Another result for cholesterol presence detection in normal eye shown as in Fig. 16 below, where the eye images in this figure shown variety of process involve from original eye until analysis to determine cholesterol presence.

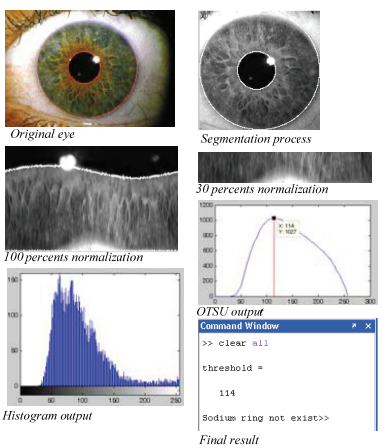

Fig. 16: Results from normal eye

The output from this experiment shown in Fig. 16 indicate the eye image have no symptom of cholesterol presence this shown in command window result "Sodium ring not exist" and the threshold value give 114 which is below the threshold value (139). This shows the iris image contain no symptom of cholesterol presence. Another result from abnormal eye image is shown in Fig.17 below. The process follows the same method as describe in above procedure.

For this image the threshold value determine is 148 which is higher than the set point 139 thus the result in command window display the message "Sodium ring had been detected", this indicate the eye encompass of cholesterol presence symptom.

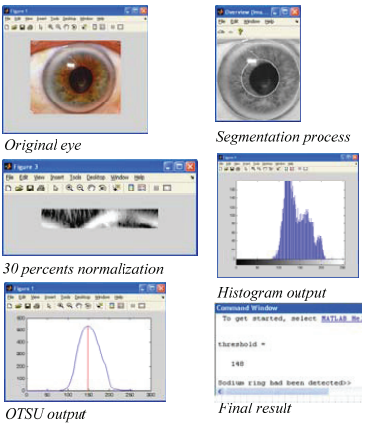

Fig. 17: Results from normal eye

VIII. CONCLUSION

This work introduces a non-invasive method and iris recognition to detect the presence of cholesterol known as hyperlipidemia by the sign of existence arcus senilis in iris pigmented. Similar opinion support by iridology practitioner call this symptom as sodium ring refer to arcus senilis sign of cardio heart diseases (CHD). The algorithm had been tested on more than 50 samples of normal and abnormal eye images; it can be conclude that the threshold boundary of the normal and problem eye is about 139.

The entire process of detecting cholesterol presence using automated program (ADCP), developed using MATLAB coding refer to Mr. Libor Masek's work. However this algorithm uses only a single method to determine the cholesterol sign i.e the arcus senilis which is using OTSU method with histogram analysis.

Other method can be used for determines the arcus senilis region such as using

neural network or sampling method for detecting either normal or diseases eye (arcus Senilis).

Secondly the improvement can be done such as using graphic user interface (GUI) for execute and displaying the result. This program also can be used to determine the eye problem due to other type of eye diseases such as cataract, glaucoma, diabetic, tumour etcetera.

ACKNOWLEDGMENT

The deepest gratitude and thanks to Universiti Teknikal Malaysia Melaka (UTeM) and Faculty Electronic and Computer Engineering (FKEKK) for supporting this publication. Thanks are also due to Mr. Libor Masek for sharing MATLAB code of Daugman's matching algorithm as public resource [5].

REFERENCES

[1] O. Thefreedictionary, "Online dictionary," Online dictionary, 1998. [Online]. Available: http://www.thefreedictionary.com/iris.

[2] D. J. Pesek and P. D, "Iridology – An Overview," North, 2010.

[3] S. C. Reddy and U. R. Rao, "Ocular complications of adult rheumatoid arthritis.," Rheumatology international, vol. 16, no. 2, pp. 49-52, Jan. 1996.

[4] G. Forbes, D. Feary, C. Savage, L. Nath, S. Church, and P. Lording, "Acute myeloid leukaemia (M6B: pure acute erythroid leukaemia) in a Thoroughbred foal.," Australian veterinary journal, vol. 89, no. 7, pp. 269-72, Jul. 2011.

[5] L. Masek, "Recognition of Human Iris Patterns for Biometric Identification," Measurement, 2003.

[6] J. Daugman, "Iris Recognition," American Scientist, vol. 89, no. 4, p. 326, 2001.

[7] J. Daugman, "How Iris Recognition Works," IEEE Transactions on Circuits and Systems for Video Technology, vol. 14, no. 1, pp. 21-30, Jan. 2004.

[8] F. L. Urbano, "Ocular Signs of Hyperlipidemia," Hospital Physician, no. November, pp. 51-54, 2001.

[9] N. Haq, M. D. Fox, A. Garton, and R. B. Northrop, "Mid Infrared Spectroscopic Absorption and Whole Blood Cholesterol," Blood, vol. i, pp. 33-34, 1991.

[10] D. Skin and C. Testing, "Issues in Emerging Health Technologies," Archives des Maladies du Coeur et des Vaisseaux, no. 34, 2002.

[11] J.-Y. Um *et.al.*, "Novel approach of molecular genetic understanding of iridology: relationship between iris constitution and angiotensin converting enzyme gene polymorphism.," The American journal of Chinese medicine, vol. 33, no. 3, pp. 501-5, Jan. 2005.

[12] H. Z. Pomerantz, "The relationship between coronary heart disease and the presence of certain physical characteristics.," Canadian Medical Association Journal, vol. 86, pp. 57-60, Jan. 1962.

[13] N. Useful and P. Harmful, "Not Useful and Potentially Harmful," vol. 118, pp. 120-121, 2000.

[14] UBIRIS Proenca, H. and Filipe, S. and Santos, J. R. and Oliveira, and L. A. } and Alexandre, "The [UBIRIS.v2]: A Database of Visible Wavelength Images Captured On-The-Move and At-A-Distance," 2010. [Online]. Available: http://iris.di.ubi.pt/ubiris2.html.

[15] UPOL, "UPOL," 2003. [Online]. Available: http://phoenix.inf.upol.cz/iris/download/.

[16] MMU, "MMU," 2005. [Online]. Available: http://pesona.mmu.edu.my/~ccteo/.

[17] CASIA, "CASIA," 2003. [Online]. Available: http://www.cbsr.ia.ac.cn/IrisDatabase.htm.

[18] T. A. Camus and R. Wildes, "Reliable and Fast Eye Finding in Close-up Images," Intelligence, 2002.

[19] W.-kin Kong and D. Zhang, "Detecting Eyelash and Reflection for Accurate Iris Segmentation," no. 852.